JOURNAL OF MATERIALS SCIENCE **39** (2004) 4131–4137

Synthesis and properties of titanium dioxide/polydimethylsiloxane hybrid particles

MASATO NAKADE, KOICHI KAMEYAMA
Research and Development Division, KOSÉ Corporation, Azusawa 1-18-4, Itabashi-ku, Tokyo 174-0051, Japan
E-mail: m-nakade@kose.co.jp

MAKOTO OGAWA
Department of Earth Sciences, Waseda University, Nishi-waseda 1-6-1, Shinjuku-ku, Tokyo 169-8050, Japan

Spherical particles of titanium dioxide and poly(dimethylsiloxane) hybrid have been synthesized from titanium tetraisopropoxide and methoxy-functionalized poly(dimethylsiloxane) by a co-precipitation method. The refractive index of the hybrid particles exhibits a linear relationship with the titanium dioxide content. These hybrid particles have elastic properties. The nano structures of the products were characterized by TEM, XRD, IR, UV-Vis. spectroscopy and HAADF-STEM. The hybrids have an islet-like nano-structure, which consisted of titanium dioxide and PDMS domains in the nanometer size range.

1. Introduction

The advantage of combining properties of organic and inorganic components in a material has been reported for developing high-performance, multi-functional materials. The syntheses of inorganic-organic hybrid materials by a wide variety of synthetic approaches have been reported, and the functions of the resulting hybrid materials have become an expanding field of investigation [1]. The sol-gel method is a promising way to access inorganic-organic hybrid materials, especially the hybrids of silica and organic polymers [2–16]. The sol-gel process, which is used mainly in inorganic polymerization reactions, is a method initially used for the preparation of inorganic materials such as glasses and ceramics. Its low-temperature processing characteristic provides unique opportunities to make inorganic-organic hybrid materials of precisely controlled composition. Due to the optical qualities, the sol-gel derived hybrids have been applied as optical materials and coating films [2, 10–16]. The properties depend on the chemical nature of their components and the nano-structure, including the interactions between the components [14]. Consequently, controlling the structures of hybrids at the nanoscopic scale, including the design of the inorganic-organic interfaces, is an important problem.

The macroscopic morphology is another key issue for the practical applications. Among possible controlled morphology, spherical particles are useful for various fields including chromatography, fine ceramics and pigments. The precipitation method has been one of the main processes to synthesize the spherical particles of inorganic materials. Toki reported the synthesis of the hybrid particles of silica and poly(vinylpyrrolidone) or poly(2-ethyloxazoline) by applying the precipitation method [17].

This paper reports the synthesis and the properties of titanium dioxide/polydimethylsiloxane (PDMS) hybrid particles. The controlled optical properties [18–22], e.g. the refractive index and the mechanical properties of the film [23–25] have previously been reported for the hybrids of organic or silicone-containing polymers and titanium dioxide. Thus, the properties of the hybrid particles of titanium dioxide and silicone are also expected to vary depend on the chemical compositions as well as the degree of hybridization. To obtain the hybrid particle with controlled macroscopic morphology, a co-precipitation technique was utilized. Furthermore, the chemical compositions of the hybrid particles were successfully controlled. The refractive index and hardness of the resulting hybrid particles were evaluated, and their nano-structures were investigated by means of spectroscopy and microscopy.

2. Experimental

2.1. Materials

Titanium tetraisopropoxide (TTP) was purchased from Wako Pure Chemical Industries (Wako 1st grade 95% + (wt)). Methoxy-functionalized PDMS

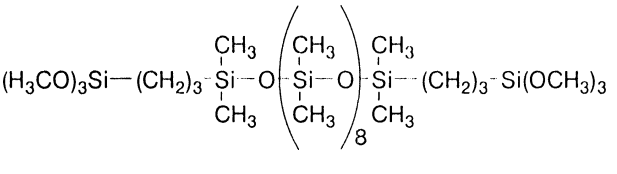

Scheme 1 Chemical structure of the methoxy-functionalized polydimethylsiloxane.

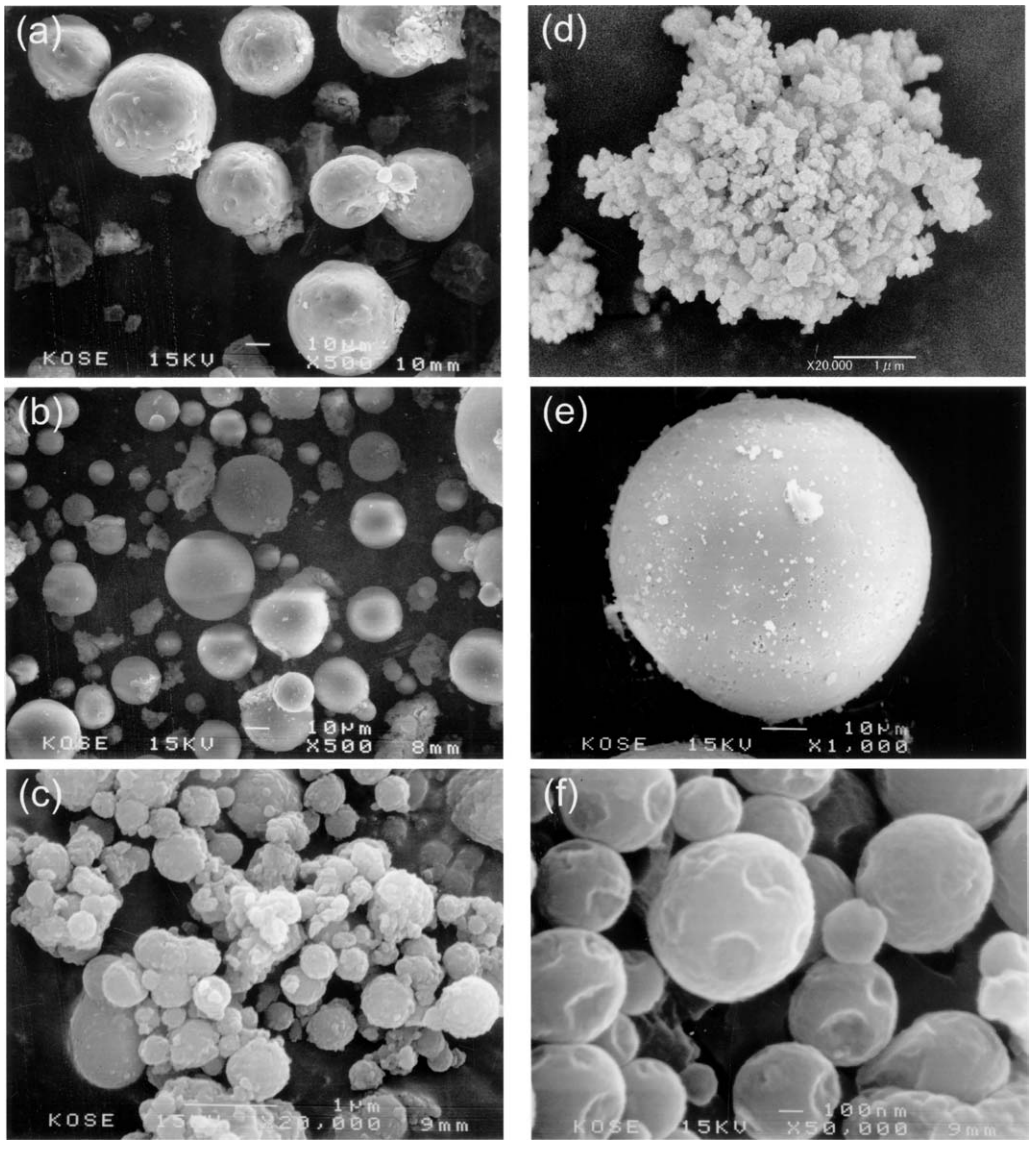

Figure 1 SEM micrographs of the TiO_2/PDMS hybrid particles. (a) T/S (2.5), (b) T/S (5), (c) T/S (10), (d) T/S (20), (e) Enlargement of (b), (f) Enlargement of (e), showing the small particles on the surface of the large particle.

(methoxy-PDMS; Scheme 1) was supplied by Shin-etsu Chemical. These chemicals were used without further purification. 2-Propanol, methanol, aqueous ammonia solution (28.0% NH_3) and hydrochloric acid were analytical grade of Kanto Chemical. Ind. Co., and they were used as received.

2.2. Synthesis of the hybrid particles

The synthesis of titanium dioxide/PDMS hybrid particles was carried out in two steps. In the first step, a transparent titania sol was prepared. Generally, when starting from titanium alkoxides for synthesis of hybrids containing titanium dioxide, additives (for example, chelating agents) are used to control the rate of hydrolysis. However, these additives may remain in the products, and they are known to affect the properties of the products [18]. For this reason, a transparent titania sol was prepared without additives according to the method reported by Wang *et al.* [22]. The titania sol was prepared by slowly adding 40 ml of 2-propanol solution containing water (1.80 g) and HCl (0.219 g) to TTP (28.4 g) at room temperature. The molar ratio of TTP, water, and HCl was 1:1:0.06. To this sol, methoxy-PDMS diluted with 20 ml of 2-propanol was added, so that a transparent titanium dioxide/PDMS hybrid sol was obtained. This hybrid sol gave a transparent and slightly-yellow xerogel, when evaporated the solvent slowly. The amount of the added methoxy PDMS varied from 5.26 to 21.0 g, as indicated in Table I.

In the second step, these sols containing titanium dioxide and oligomeric PDMS were co-hydrolyzed and co-condensed in an alkaline methanol solution. These sols were added, under vigorous stirring, to a mixture of methanol (600 ml), distilled water (180 ml) and aqueous ammonia solution (20 ml), so that a

TABLE I Sample ID and chemical compositions of the products

Sample ID	Molar ratio of starting materials $Ti(OPr)_4$/Methoxy-PDMS (atomic ratio; Ti/Si)	Atomic ratio; Ti/Si (experimental value)
T/S (2.5)	2.5/1 (1/4.8)	1/3.9
T/S (5)	5/1 (1/2.4)	1/2.2
T/S (10)	10/1 (1/1.2)	1/1.3
T/S (20)	20/1 (1/0.6)	1/0.53

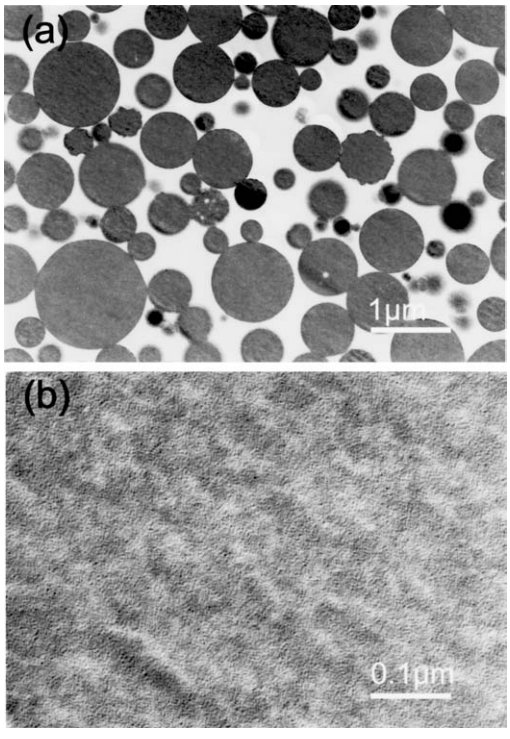

Figure 2 (a) Shows TEM image of the ultra thin section of small particles in T/S (5). (b) Enlargement of (a).

rapid precipitation took place and turbid dispersion was obtained. After the reaction for several minutes, the precipitates—the hybrid particles—were collected by centrifugation (3000 rpm) and subsequently washed with an appropriate amount of 2-propanol and dried at 100°C. The dried samples were fine white powder.

2.3. Characterization

The images of the particles were obtained by scanning electron microscopy (SEM) (JEOL, JSM-6301F) equipped with an energy-dispersive X-ray spectroscopy (EDS) system and transmission electron microscopy (TEM) (JEOL, JEM-1200 EXII, 80 kV). For SEM observation, samples were coated with platinum by sputtering. For TEM observation, ultra-thin sections of the particles were prepared by ultra microtome (Reichert-Jung, Super Nova). The chemical composition was determined for both the bulk sample and the specific area of a particle by EDS. A disk-shaped pellet of the sample was prepared for the bulk analysis by pellet dies and a hydraulic press, and then the pellet was coated with carbon under high vacuum. For the chemical analysis of the individual particle, the sample preparation was same as the morphological observation.

The immersion method was used to determine the refractive indices of the hybrid particles with varied titanium dioxide/PDMS ratios. The series of hybrid particles was dispersed in media with various refractive indices, and the refractive indices of the particles were estimated by the transparencies of the dispersions observed with the naked eye.

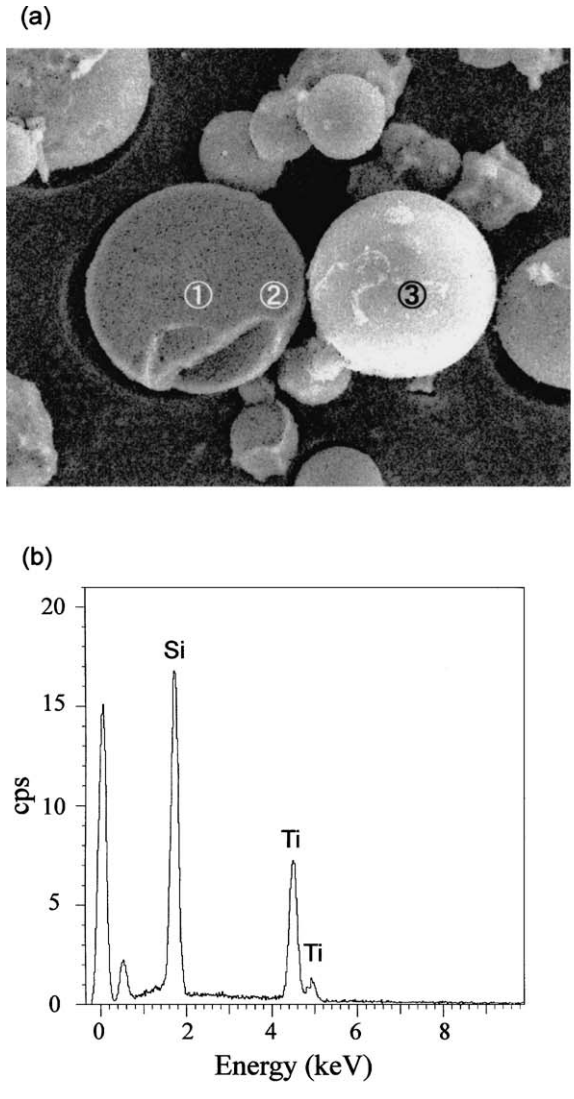

(c)

Measuring Point	*Atomic Ratio, Ti/Si*
Point ①	1/1.9
Point ②	1/1.9
Point ③	1/1.9

Figure 3 SEM/EDS measurement of the TiO_2/PDMS hybrid particle T/S(5). (a) SEM micrograph and the measuring points. (b) EDS spectrum at Point ①. (c) Chemical composition at the measuring points.

To compare the mechanical properties with those of a titanium dioxide particle, the relationship between the displacement and the load against individual hybrid particles was measured with a microcompression-testing instrument (Shimadzu MCTM). A particle was put on the stage, and then pressed by a small indentator under the microscope observation.

X-Ray diffraction (XRD) patterns (in the $2\theta = 5$–60° range) were obtained with an X-ray diffractometer (RIGAKU MultiFlex), employing Cu K_α radiation and a graphite monochromator. Fourier transform infrared (FT-IR) spectra were obtained with a spectrophotometer (JASCO 660 Plus) collecting 64 scans in the range of 4000–400 cm^{-1} on KBr disks with 2 cm^{-1}

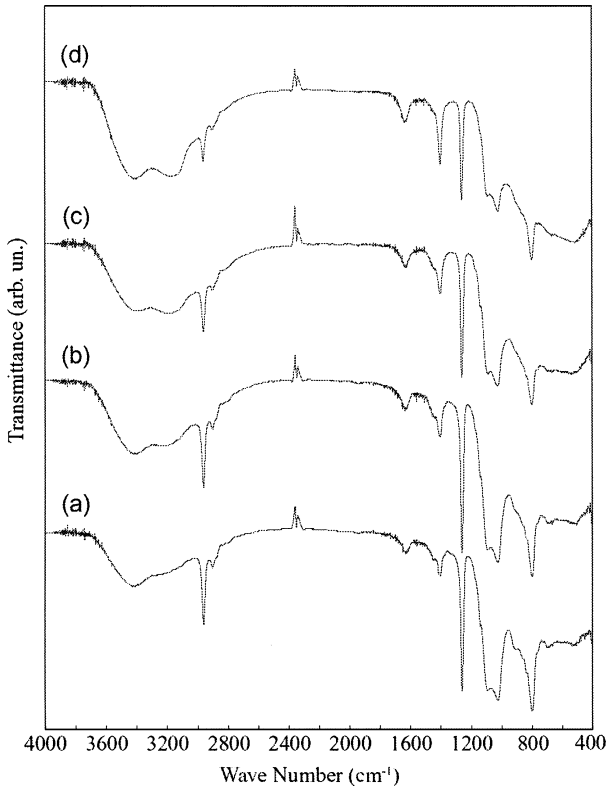

Figure 4 IR spectra of the TiO_2/PDMS hybrid particles. (a) T/S (2.5), (b) T/S (5), (c) T/S (10) and (d) T/S (20).

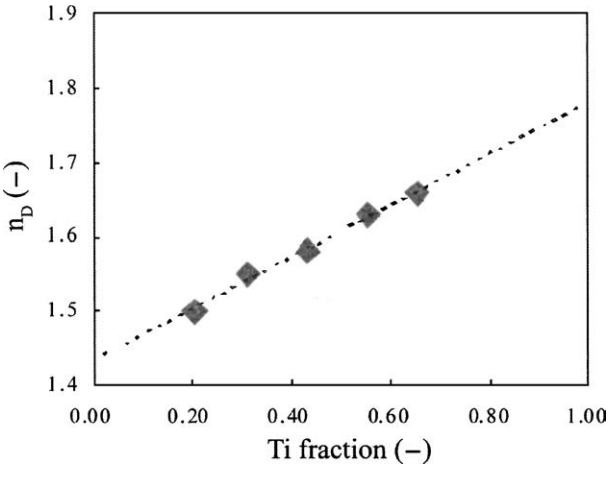

Figure 5 Refractive index of the TiO_2/PDMS hybrid particles.

resolution. Ultraviolet and visible (UV-Vis.) diffuse reflectance spectra of the samples were recorded on a UV-Vis. spectrometer equipped with an integrating sphere (JASCO ISN-470) using a cell holder with a quartz window. The nano-structure of the hybrid particle in the present study was investigated by means of high-angle annular dark field scanning transmission electron microscopy (HAADFSTEM) equipped with an EDS system (JEOL, JEM-2010F) on the ultra thin section of the hybrid particle. The image acquired by a HAADF detector in the scanning mode of a transmission electron microscope with a finely focused electron probe yields intensity distributions depending on the atomic number (Z) at a nano-scale.

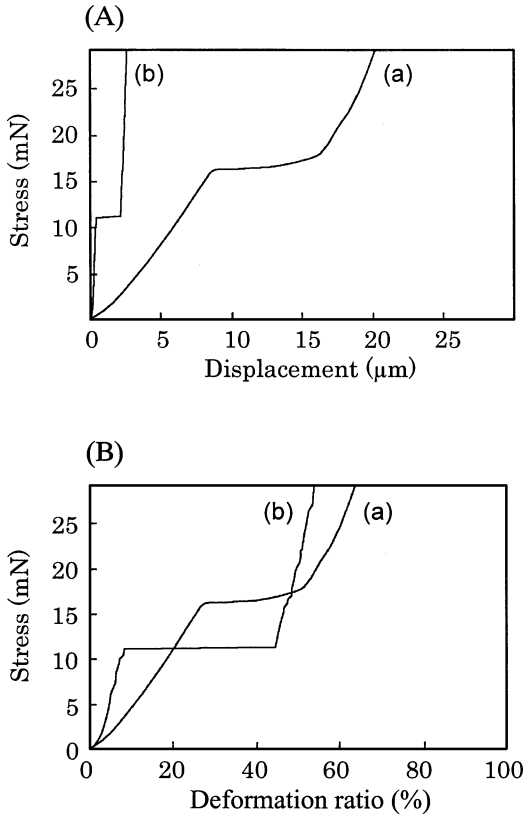

Figure 6 Displacement measurement of a particle. (a) T/S (5); 28.4 μm, (b) TiO_2; 5.25 μm in diameter; (A) Stress vs. Displacement value, and (B) Stress vs. Deformation ratio.

3. Results and discussion

3.1. Synthesis of titanium dioxide/PDMS hybrid particles

The identifications of the products and their chemical compositions are shown in Table I. These compositions were obtained by SEM-EDS measurement and the ZAF correction method (where Z is the correction due to the atomic number of the matrix, A is the correction of photoelectric absorption factor of X-rays in the specimen, and F is the fluorescence correction factor). The results were semi-quantitative. However, they demonstrated that the chemical compositions of the final products corresponded to the Ti/Si ratios of the starting materials.

The SEM observations showed that the particles had nearly spherical shapes except for T/S (20), and their size depended on the TTP/methoxy-PDMS ratio as shown in Fig. 1. For T/S (5), for example, the particle was several tens of micrometers in diameter. On the surface of these large particles, there were submicron spherical particles of about 0.5 μm in diameter. The formation of the large particles was caused by interfacial tension due to the low solubility of the hybrid sol. However, the reason why spherical particles of different sizes are generated simultaneously is uncertain at the present stage. For T/S (10), as opposed to T/S (5), the average particle diameter of the spherical particle was around 0.5 μm. It was supposed that the difference in morphology between T/S (5) and T/S (10) was derived from the difference of the reaction rate and/or solubility of the sols to the alkaline methanol solution. Because the solubility of the sol to the alkaline-methanol

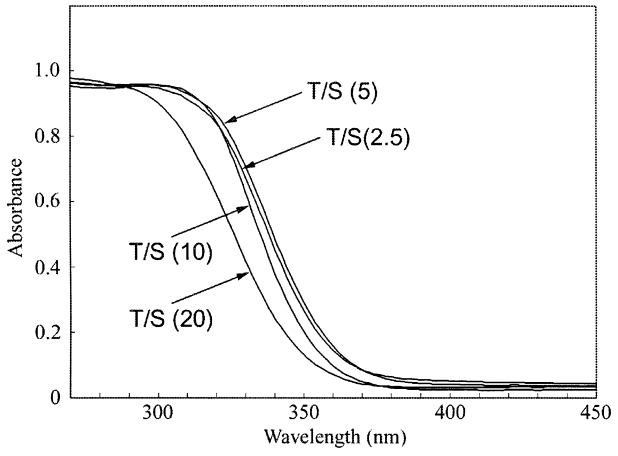

Figure 7 UV-Vis. spectra of the TiO_2/PDMS hybrid particles.

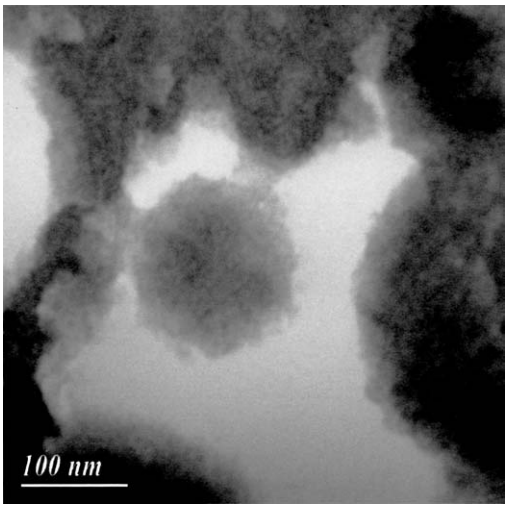

Figure 8 STEM image of the ultra thin section of T/S (5).

solution is decreased as the ratio of the silicone increases in the sol, it is conceivable that big droplets will be easy to generate by the interfacial tension. The reactivity of the silicone-rich sol is relatively low because the reactivity of the alkoxy-silicone is lower than that of titanium alkoxide. In the case of T/S (5), the reaction will not complete just after the contact between the sol and the alkaline-methanol solution, which results in the generation of large droplets of the sol.

Fig. 2 shows TEM observation of the cross section of the small particles for T/S (5). These TEM micrographs demonstrate that there is no recognizable phase separation.

The chemical compositions of the particles were determined by means of SEM equipped with EDS to confirm the homogeneity in the composition. The presence of Ti and Si was detected for all the observed particles, and the Ti/Si ratios were constant. In the case of T/S (5), a cross section of a single particle was also examined. There was no difference in the ratio of Ti/Si ratio between the core area and the near-surface are of the particle (Fig. 3). These results demonstrated that titanium dioxide and PDMS were hybridized at a nanometer scale.

3.2. Refractive index of the hybrid particle

The refractive indices of the particles were determined by the immersion method. It has been reported that the refractive index of the hybrid film derived from titanium dioxide as the inorganic component and PDMS, poly(arylene ether ketone) (PEK) or poly(arylene ether sulfone) (PSF) as the organic component increased linearly with increasing Ti fraction [19, 21]. The refractive indices of the present hybrid particles also increased with increasing the Ti fraction. There was a linear relationship between the refractive index vs. fraction of Ti as shown in Fig. 5. This means that the optical properties of the hybrid particle can be controlled by varying the composition of the starting materials [18, 26, 27].

3.3. Mechanical properties of the hybrid particle

For T/S (5), the deformation of a particle was measured by the microcompression testing instrument to evaluate the mechanical properties. As a control, a single crystal titanium dioxide particle with 4.84 μm in diameter on average was used. Fig. 6A shows the relationship between load and displacement when a particle on the stage was pressed by the indentator. The mean displacement until the particle collapsed was 8.4 μm for the hybrid particle (mean diameter; 26.0 μm), while it was 0.53 μm for the titanium dioxide particle (mean diameter; 4.84 μm), and the compressive force at the collapse point for the hybrid particle was larger than for the titanium dioxide particle. The curve of the hybrid particle showed that it has elastic properties, while titanium dioxide was rigid. To correct the difference of particle size between titanium dioxide and the hybrid, the deformation ratio is plotted as abscissa. Fig. 6B shows that the deformation ratio at the collapse point is 32% for the hybrid particle and 11% for the titanium dioxide particle. This result revealed that the hybrid particle was flexible originating from PDMS.

3.4. Structural characterization

The XRD patterns indicate that the hybrids were amorphous, which was consistent with the TEM observations. In the IR spectrum, the absorption bands due to silicone appear at 1261, 1089, and 1022 cm^{-1} (Fig. 4). These three bands are assigned to Si-CH_3 bending vibrations (1261 cm^{-1}) and to Si-O stretching vibrations (1089 and 1022 cm^{-1}) typical of PDMS units. As a whole, the profile of the spectrum was an overlapping of the separate absorptions due to titanium dioxide and PDMS. With the increase in the titanium content, the absorption band at around 3200 cm^{-1} due to Ti—OH and the broad absorption band at the low wavenumber area due to an envelope of Ti—O—Ti bonds become more intense as shown in Fig. 4. In the previous study of the poly(tetramethylene oxide)-titania hybrid derived from triethoxysilane end-capped poly(tetramethylene oxide) oligomer, an absorption band at 920 cm^{-1} was observed and ascribed to Ti—O—Si [18]. Such absorption band was not observed in the present system. The absence of the band at 920 cm^{-1} can be explained by the small amount of the Ti—O—Si bond and/or the absence of Ti—O—Si linkage at the TiO_2/PDMS interface.

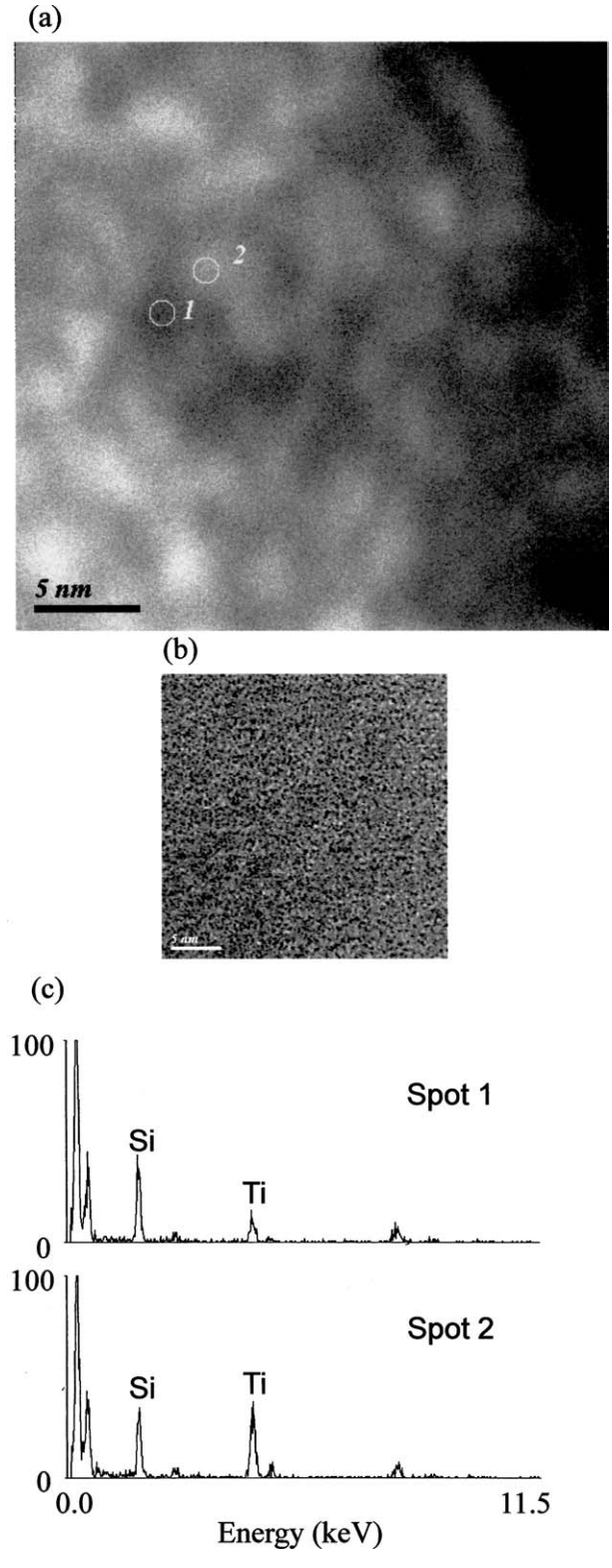

Figure 9 STEM/EDS measurement of T/S (5). (a) HAADF image with EDS measuring spots (b) BF image. (c) EDS spectrum at the measuring spots.

Fig. 7 shows the UV-Vis. diffuse reflectance spectra of the hybrid particles. The hybrid particles were transparent in the visible wavelength region. The absorption edge for T/S (2.5), T/S (5), T/S (10) and T/S (20) appear at about 360 nm, 360 nm, 355 nm and 350 nm respectively, which exhibit blue shifts relative to that of rutile (410 nm). This observation suggests that the sizes of the titanium dioxide phases are small so that a quantum size effect causes the spectral blue shift. It is obvious that the absorption edge shifts to shorter wavelength regions as the titanium content increased, namely, as the particle size becomes smaller. It is presumed that the degree of blue shift for different compositions reflects the difference in the size or the chemical environment of the TiO_2 nano-domains [29, 30].

Figs 8 and 9 show STEM images of the ultra thin section of T/S (5). Fig. 8 shows a low magnification image, and Fig. 9a and b show magnified images obtained from the same area. Fig. 9a and b show HAADF (Z-contrast) and blight-field images of the hybrid particle. The thin part at the edge of the particle was observed to eliminate the influence of the thickness. Specimens with apparent thickness variations may display a high intensity in thicker areas, and in such specimens the HAADF signal is not necessarily due to a high atomic number. Fig. 9b exhibits an image typical to amorphous materials with no obvious contrast. On the other hand, Fig. 9a clearly demonstrates the contrast due to the nano-structure of the hybrid. In the HAADF image, highlighted areas show the positions of relatively heavy atom. Therefore, the highlighted contrast in Fig. 9a shows titanium dioxide domains, which have islet-like structures which are about 4 nm in diameter. To confirm this observation, the chemical composition was analyzed by the EDS system. Measuring on the dark area (Spot 1) and the highlighted area (Spot 2), it was confirmed that the peak due to Ti was relatively intense in Spot 2 (Fig. 9c). These results revealed that the hybrid particle had an islet-like nano-structure, which consisted of titanium dioxide and PDMS nano-domains. These EDS spectra included signals from the vertical dimension of the specimen so that there was a peak due to Si even in the highlighted area. This conclusion agreed with the results of IR and UV-Vis. spectroscopy as mentioned above.

4. Conclusions

Spherical particles of titanium dioxide/PDMS hybrid with the diameter of 50 μm were successfully synthesized from titanium tetraisopropoxide and methoxy-functionalized PDMS by co-precipitation method. Nano-scale hybridization between titanium dioxide and PDMS was confirmed by TEM observations. The hybrid particle had an islet-like nano-structure, which consisted of titanium dioxide and PDMS domains of a nano meter size. The refractive index of the hybrid particle could be controlled by varying the titanium dioxide/PDMS ratio. Moreover, the hybrid particle had elastic properties originated from the PDMS component.

References

1. Special issue on "Organic-Inorganic Nanocomposite Materials," *Chem. Mater.* **13** (2001) 10.
2. G. PHILIPP and H. SCHMIDT, *J. Non-Cryst. Solids* **63** (1984) 283.
3. H. SCHMIDT, *ibid.* **73** (1985) 681.
4. D. RAVAINE, A. SEMINEL, Y. CHARBOUILLOT and M. VINCENS, *ibid.* **82** (1986) 210.
5. C. ROSCHER and M. POPALL, *Mater. Res. Soc. Symp. Proc.* **435** (1986) 547.

6. H. HUANG, B. ORLER and G. L. WILKES, *Polym. Bull.* **14** (1985) 557.
7. G. L. WILKES, B. ORLER and H. HUANG, *Poly. Prep.* **26** (1985) 300.
8. J. E. MARK and C. C. SUN, *Polym. Bull.* **18** (1987) 259.
9. S. KOJIYA, *J. Non-Cryst. Solids* **119** (1990) 132.
10. S. DIRE, F. BOBONNEAU, C. SANCHEZ and J. LIVAGE, *J. Mater. Chem.* **2** (1992) 239.
11. H. SCHMIDT and H. J. WOLTER, *J. Non-Cryst. Solids* **121** (1990) 42810.
12. S. MOTAKEF, T. SURATWALA, R. L. RONCONE, J. M. BOULTON, G. TEOWEE, G. F. NEILSON and D. R. UHLMANN, *ibid.* **178** (1994) 31.
13. H. SCHMIDT, *ibid.* **178** (1994) 302.
14. B. M. NOVAK, *Adv. Mate.* **5** (1993) 422.
15. H. HUANG, B. ORLER and G. L. WILKES, *Macromolecules* **20** (1987) 1322.
16. F. BABONNEAU, *Polyhedron* **8** (1994) 1123.
17. M. TOKI, *J. Sol-Gel Science and Tech.* **2** (1994) 97.
18. B. WANG, A. B. BRENNAN, H. HUANG and G. L. WILKES, *J. Macromol. Sci.-Chem.* **A27** (1990) 1477.
19. S. S. JOARDER, M. A. JONES and T. C. WARD, *Polym. Mater. Sci. Eng.* **67** (1992) 254.
20. S. DIRE, F. BABONNEAU, G. CARTURAN and J. LIVAGE, *J. Non-Cryst. Solids* **147/148** (1992) 62.
21. B. WANG, G. L. WILKES, J. C. HEDRICK, S. C. LIPTAK and J. E. McGRATH, *Macromolecules* **24** (1991) 3449.
22. B. WANG and G. L. WILKES, *J. Polym. Sci.: Part A: Polym. Chem.* **29** (1991) 905.
23. N. YAMADA, I. YOSHINAGA and S. KATAYAMA, *J. Mater. Chem.* **7/8** (1997) 1491.
24. R. H. GLASER and G. L. WILKES, *Polym. Bull.* **19** (1988) 51.
25. D. W. McCARTHY, J. E. MARK, S. J. CLARSON and D. W. SCHAEFER, *J. Polym. Sci.: Part B*, **36** (1998) 1191.
26. B. LITNER, N. ARFSTEN, H. DISLICH, H. SCHMIDT, G. PHILIPP and B. SEIFERLING, *J. Non-Cryst. Solids* **100** (1988) 378.
27. Y. WEI, D. YANG, L. TANG and M. G. K. HUTCHINS, *J. Mater. Res.* **8** (1993) 1143.
28. V. A. ZEITLER and C. A. BROWN, *J. Phys. Chem.* **61** (1957) 1174.
29. L. E. BRUS, *J. Chem. Phys.* **79** (1983) 5566.
30. H. WELLER, *Angew. Chem. Int. Ed. Eng.* **32** (1993) 41.

Received 18 August 2003
and accepted 18 March 2004